Test of the predictability of PI method on the Tohoku M_w9.0 earthquake

*Yongxian Zhang[1], Cheng Song[2], Caiyun Xia[3], Shengfeng Zhang[4]

1. China Earthquake Networks Center, 2. Institute of Earthquake Science, China Earthquake Administration, 3. Liaoning Earthquake Administration, 4. Institute of Geophysics, China Earthquake Administration

In this research, the local area (32.0˚~46.0˚N, 136.0˚~148.0˚E) including most of Japan was chosen to be the study region for verifying the predictability of the pattern informatics (PI) method under different models with different parameters using the receiver-operating characteristic (ROC) curve test and *R* score test. Pattern Informatics (PI) method was applied to the retrospective study on the forecasting of large earthquakes especially the Tohoku M_w9.0 earthquake in this region. Different forecasting maps with different calculating parameters were obtained. The main calculating parameters were respectively the grid size of 0.5˚×0.5˚ or 1.0˚×1.0˚ and forecasting window lengths from 5 to 10 years. The results showed that in most of the models, the hotspots were in its Moore neighborhood grids or its epicentral grid in the forecasting windows containing the M_w9.0 Tohoku earthquake, which suggests that the PI method could forecast the Tohoku M_w9.0 earthquake. The results also showed that under the ROC test and *R* score test the models with larger grid size (1.0˚×1.0˚) and longer forecasting window length (7~10 years), the forecasting effect were better.

Keywords: PI method, Tohoku Mw9.0 earthquake, predictability, ROC test, R score test

Nowcasting Global Earthquakes

*John B Rundle[1], Molly Luginbuhl[1], Alexis Giguerre[1], Donald L Turcotte[2]

1. Department of Physics, University of California, Davis, California, USA 95616, 2. Department of Earth and Planetary Science, University of California, Davis, California, USA 95616

The term "nowcasting" refers to the estimation of the current uncertain state of a dynamical system, whereas "forecasting" is a calculation of probabilities of future state(s). Nowcasting is a term that originated in economics and finance, referring to the process of determining the uncertain state of the economy or markets at the current time by indirect means.
We have applied this idea to seismically active regions, where the goal is to determine the current state of a system of faults, and its current level of progress through the earthquake cycle (http://onlinelibrary.wiley.com/doi/10.1002/2016EA000185/full).
We wish to estimate how far the fault system has progressed through the "cycle" of large recurring earthquakes. We use the global catalog of earthquakes, using "small" earthquakes to determine the level of hazard from "large" earthquakes in the region. As an application, we can define a small region around major global cities, for example a "small" circle of radius 150 km and a depth of 100 km, as well as a "large" earthquake magnitude, for example M6.0. Also, the region of influence of such earthquakes is roughly 150 km radius x 100 km depth, which is the reason these values were selected.
The statistics are computed from a "large" 10^{o} x 10^{o} region surrounding the "small" 150 x 100 km circle. The current count of earthquakes that is used to compute the nowcast is obtained from small earthquakes in the small region. The basic assumption is that both the "large" and "small" regions are characterized by the same Gutenberg-Richter magnitude frequency statistics.
If one defines a "model" as a calculation system in which there exist free parameters that must be optimally fit to data, then it can be said that there is no model involved in our nowcasting analysis. Our methods involve only plotting and interpreting data, once the magnitude threshold and spatial region have been selected.
We have used these techniques to compute the relative nowcast rankings of large global cities at risk for damaging earthquakes. In this talk we discuss these rankings. We also discuss the results of sensitivity analyses of the rankings to variations in the selected magnitude, small and large regions.

Keywords: Global Earthquakes, Nowcasting, Sensitivity testing

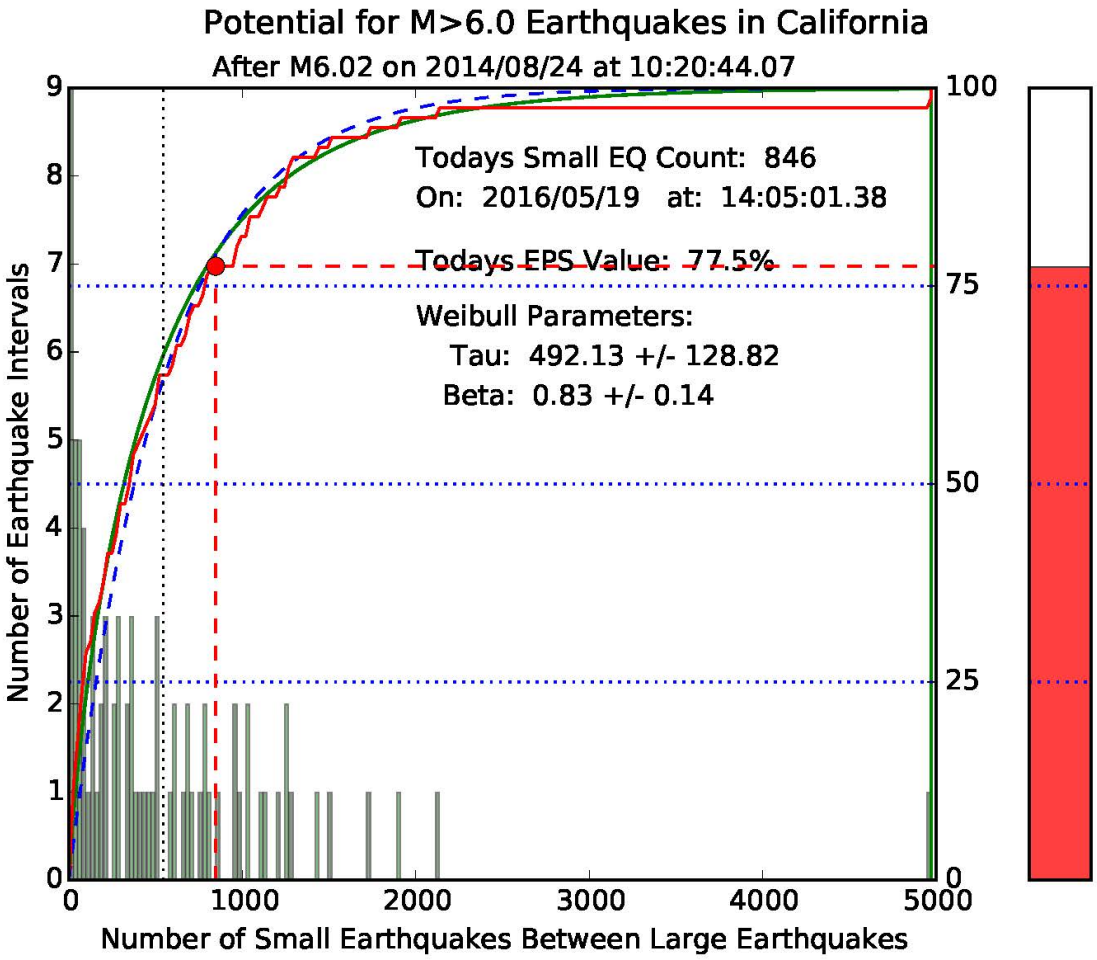

Detailed inversion of a shallow slow slip event at the Hikurangi subduction zone, New Zealand, using numerical Green's functions and absolute pressure gauge data

*Charles A Williams[1], Laura M Wallace[1], Spahr C Webb[2], Yoshihiro Ito[3], Kimihiro Mochizuki[4], Ryota Hino[5], Stuart Henrys[1]

1. GNS Science, 2. Lamont-Doherty Earth Observatory, 3. Disaster Prevention Research Institute, 4. Earthquake Research Institute, 5. Tohoku University

Slow slip events (SSEs) have been observed throughout the world, and the existence of these events has fundamentally altered our understanding of the possible ranges of slip behavior at subduction plate boundaries. SSEs are typically observed via continuous GPS (cGPS) observations. Although much has been learned in recent years, the slip distributions for shallow SSEs are still poorly understood due to the lack of offshore data to constrain the slip estimates. Most importantly, it has been difficult to determine whether shallow SSEs extend to the trench, or whether they terminate at some distance inboard of the trench. Constraining the slip distribution is critical to our understanding of the physics underlying SSEs.

Recently, absolute pressure gauges (APGs) were deployed offshore near Gisborne, New Zealand, as part of the HOBITSS experiment, capturing a SSE event during September and October 2014. The APGs provide a record of vertical deformation during the event, allowing much better constraints on the offshore slip distribution. Initial inversions using an elastic half-space model based on these observations indicate that slip occurred within 2 km of the trench. We here describe a more detailed inversion procedure where we include the effects of detailed fault geometry, bathymetry/topography, and material property variations to provide a more accurate estimate of the slip distribution during this event. We use the PyLith finite element code to generate Green's functions for use in our inversions. We find that inversions that take into account material property variations require larger amounts of slip, with predicted seismic potencies approximately 40% greater than homogeneous models.

Keywords: Slow slip, Hikurangi, Inversion, Numerical Green's functions, Absolute pressure gauge, Finite element

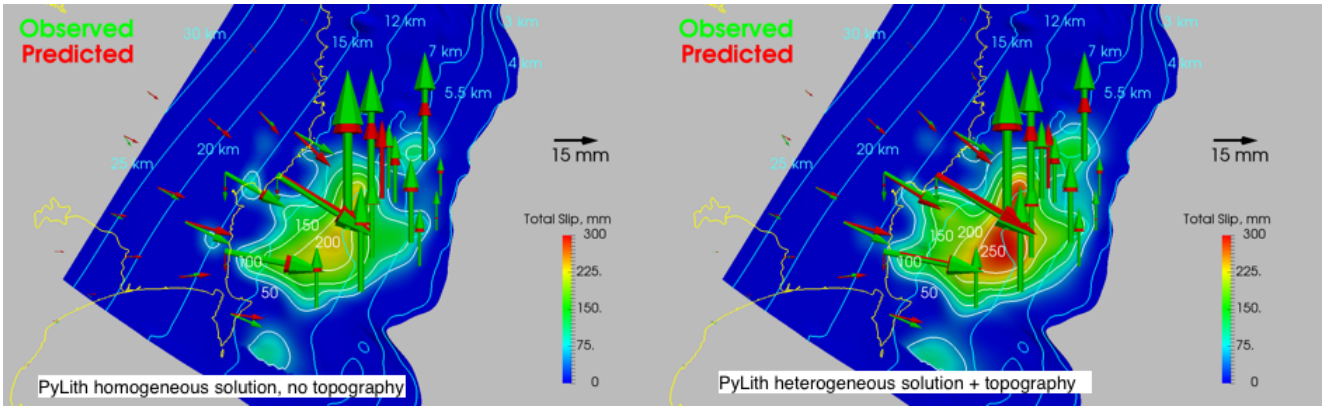

The 12 September 2016 M_L 5.8 Gyeongju, Korea, earthquake: Observation and questions

*Tae-Seob Kang[1], Kwang-Hee Kim[2], Junkee Rhie[3], Younghee Kim[3]

1. Division of Earth Environmental System Science, Pukyong National University, 2. Department of Geological Science, Pusan National University, 3. School of Earth and Environmental Sciences, Seoul National University

The M_L 5.8 earthquake in Gyeongju, southeastern Korea, on September 12, 2016 11:32:54 (UTC) was the largest earthquake on the Korean Peninsula since instrumental monitoring began in 1978. It was preceded by an M_L 5.1 foreshock and is being followed by numerous aftershocks. Within an hour of the mainshock, the first temporary seismic station to monitor aftershocks was installed at about 1.5 km east of the announced epicenter. The temporary seismic network consists of 27 stations equipped with broadband sensors covering an area of about 38 x 32 km^2 in the mainshock region. This is the first high-density aftershock monitoring array in the Korean Peninsula. Initial results, using data from both the regional seismic networks and the aftershock monitoring array, indicate that earthquakes during the first 10 days following the mainshock are related to the Yangsan Fault System. The 2016 Gyeongju events have now become forceful reminders that earthquakes have occurred in the past and can hit the region again at any time. These earthquakes provide an opportunity to reaffirm aspects already known based on evidence from both historical (literature) and seismological data. Moreover, the occurrence of the 2016 Gyeongju earthquakes has motivated more detailed studies of the Yangsan Fault System and a reexamination of the previously held consensus regarding the fault system. The most frequently asked questions during the Gyeongju earthquake crisis are as follows: Are there any active faults in the source area? Which faults are responsible for the mainshock–aftershock sequence? Is the Yangsan fault active? Is it possible to release information regarding impending earthquake activity? How long will the aftershocks continue? What is the next earthquake scenario and how to model it? These issues will be discussed on the basis of the aftershock monitoring data.

Keywords: Gyeongju, Korea, earthquake, responsible fault, future earthquake scenario

Dynamic Faulting Simulation with Cellular Automaton Model

*How-wei Chen[1]

1. Institute of Geophysics, National Central University, Taiwan, ROC

Earthquake dynamics are believed to exhibit self-organized criticality (SOC). The apparent unrest of dynamic stress changes of the crust to stress perturbations exhibits similar SOC behavior. Cellular Automaton Model (CAM) is implemented in simulating dynamic faulting processes. Early stage investigation aims in probing system dynamics by seeking any available simulation schemes including granular material, lattice-gas and lattice-solid approaches. The simulation can be realized through iterative application of rules that encapsulate the essential physics of the system by allowing uniform stress increment but rupture can be initiated and re-distributed fractally depends on the pre-defined rock strength. Automata rules control the stress concentrations that form ahead of growing ruptures and can be physically justified by assuming that failed cells have not yet healed and thus cannot support stress. We assume ruptures occur instantaneously under two distinct timescales - tectonic loading and rupture timescales. The occurrence of the faulting/fracturing can be modeled base on the dispassion (relaxation) factor and stress transfer ratio that controls the onset of instability and size of nucleation zone. Only fractional part of stress on the failing cell is redistributed to mimic dissipation where energy is lost for fracture opening, generation of seismic waves and heat generation. CAMs allow cells and eight nearest neighbors to fail repeatedly or only fail once in a single event. The event size corresponds to the total number of cells failed in a single step. The heterogeneous automaton allows redistributes stress to the unbroken nearest neighbors and hence produce more realistic stress concentrations. A Large event can be initiated from many small ones which expand as the result of interactions between tectonic loading, stress concentration, growing of rupture-front, broken or unbroken cells and local variations in fault strength. The distribution of rock strength can be homogeneous, random or fractal. No additional increment of stress is added until after rupture has ended. Spatial and temporal power-laws which statistically exhibit magnitude-frequency (size-number) distributions can be analysis from synthesized earthquake catalogs. More complex fault models to describe the geometry of nature faults can be characterized by fractal statistics with different scales.
CAM simulation encapsulates the essential physics of the system. The apparent sensitivity of crust to small stress perturbations and the occurrence of triggered earthquakes suggest that the Earth’s crust behaves similarly critical. The distribution of rock strength can be homogeneous, random or fractal. The faults are zones of weakness within the crust and individual faults may have strength fluctuations due to short-range, local variations in pore pressure and surface roughness. Alternatively, long-range elastic/visco-elastic interactions can be incorporated as well. The fault strength with surface roughness can be described with fractal dimension of 2.3. The accumulated stress is distributed to its eight surrounding neighbors with the pre-defined dispassion factor and stress transfer ratio. Tectonic loading can be uniform, random or fractal too. Cellular automaton models allow cells and eight nearest neighbors to fail repeatedly or only fail once in a single event. The heterogeneous automaton allows redistributes stress to the unbroken nearest neighbors and hence produce more realistic stress concentrations. Automata rules control the stress concentrations that form ahead of growing ruptures and can be physically justified by assuming that failed cells have not yet healed and thus cannot support stress. Only 75% of stress on the failing cell is redistributed to mimic dissipation (relaxation) where energy is lost to seismic waves and heat generation.

Keywords: Cellular automaton, lattice solid, dynamic rupture, numerical modeling, instability, self-organized criticality (SOC)

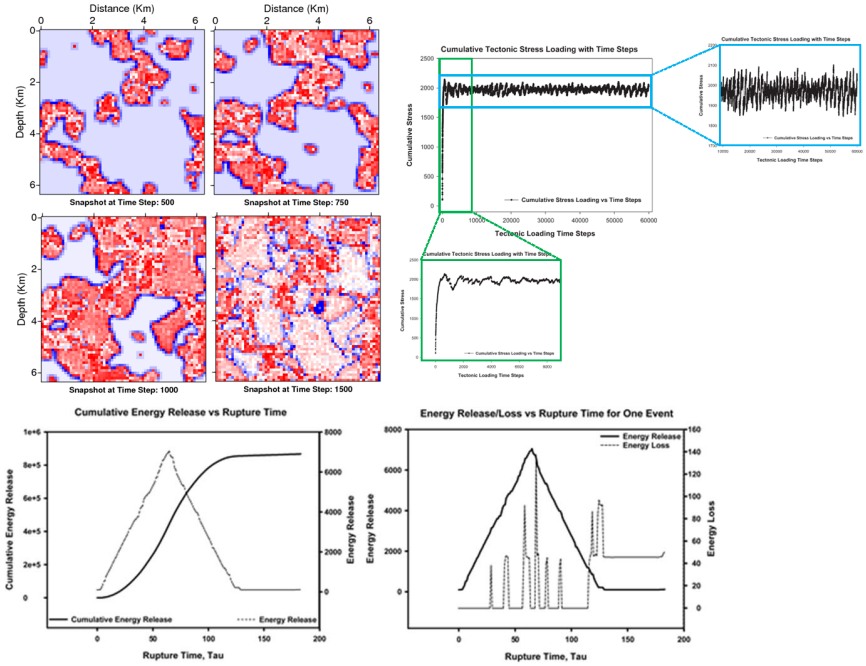

Conceptual Model for Precursory Slow Slip and Foreshocks based on the Balance of Stiffness on and around the Fault

*Eiichi Fukuyama[1], Futoshi Yamashita[1], Shiqing Xu[1], Shigeru Takizawa[1], Kazuo Mizoguchi[1,2], Hironori Kawakata[1,3]

1. National Research Institute for Earth Science and Disaster Prevention, 2. Central Research Institute of Electric Power Industry, 3. Ristumeikan University

We propose a conceptual model to understand the occurrence of precursory slow slip and foreshocks, both of which may occur prior to the mainshock. First, we summarize our experimental results of large-scale bi-axial shear friction experiments using the NIED large-scale shaking table (e.g. Fukuyama et al., 2014, Yamashita et al., 2015). In a series of experiments using an Indian metagabbro sample whose nominal slip area was 1.5m long and 0.1m wide, precursory slow slip events occurred in most cases but foreshocks were only observed under certain conditions related to the fault surface damage. When foreshocks occurred, they initiated inside the slow slip area and both coexisted. In addition, from the hypocenter distribution of foreshocks and the observation of the fault damage evolution, foreshocks tend to be initiated at the edge of grooves on the fault surface. To understand the observation described above, we shall follow the idea of Leeman et al. (2016) and Kilgore et al (2017), where the balance between the stiffness of the apparatus and that of fault surface controls. Leeman et al. (2016) varied the fault stiffness by changing the amount of normal stress while Kilgore et al (2017) varied the apparatus stiffness using springs with different elastic constants. The evolution of fault damages could be related to the apparent change in the b-a value in rate- and state- dependent friction regime (Beeler et al., 1996, Urata et al., 2016). As fault damage evolves, apparent b-a value increases. Under steady state conditions, b-a value is proportional to the fault stiffness (if positive). And we could assume that the apparatus stiffness remain constant during the episodes. Therefore, we could say that slow slip occurs where the fault stiffness is smaller than the apparatus stiffness and foreshocks occur where the fault stiffness is larger than the apparatus stiffness. In addition, Yamashita et al (2015) showed a heterogeneous distribution of local normal stress on the fault surface, especially around the grooves, and Leeman et al. (2016) showed that normal stress is also proportional to the fault stiffness. These heterogeneous distributions of normal stress and friction parameters may also cause a coexistence of slow slip and foreshocks, since the groove distribution is not uniform on the fault. In nature, stiffness of the apparatus corresponds to the stiffness of the surrounding materials of the fault. Precursory slow slip events and foreshocks can be understood based on the differences in stiffness of the fault and surrounding materials.

References:
Beeler et al. (1996) J. Geophys. Res., doi:10.1029/96JB00411
Fukuyama et al. (2014) NIED Report, http://dil-opac.bosai.go.jp/publication/nied_report/PDF/81/81-3fukuyama.pdf
Kilgore et al (2017) AGU Monograph, in press.
Leeman et al. (2016) Nature Comm., doi:10.1038/ncomms11104
Urata et al. (2016) Pure Appl. Geophys., doi:10.1007/s00024-016-1422-9
Yamashita, et al. (2015) Nature, doi:10.1038/nature16138

Keywords: Slow slip, Foreshock

Comparison of the initial rupture processes between the M_w 6.2 mainshock and the M_w 4.1 largest foreshock of the central Tottori earthquake on October 21, 2016

*Shunta Noda[1], William L. Ellsworth[2]

1. Railway Technical Research Institute, 2. Stanford University

It is one of the essential questions in seismology whether or not the rupture termination of an earthquake is deterministic at the time of initiation (e.g., Iio, 2009). To investigate this issue, Noda and Ellsworth (2016, GRL) statistically characterized initial P waves using Japanese K-NET dataset. They concluded that the P-wave displacement began in a similar way at the onset and departed from the similarity earlier for smaller events in the magnitude range up to M_w 7. The departure time (T_{dp}) is approximately 30% of typical source duration, implying a connection between initial rupture process and the final earthquake size. To discuss this, we model slip histories during the initial stages of the M_w 6.2 central Tottori earthquake on October 21, 2016 in Japan and its largest foreshock of M_w 4.1 that occurred about two hours before the mainshock. Because these hypocenters are co-located and the focal mechanisms are identical according to the JMA catalog, we invert them using the same empirical Green's functions derived from other foreshocks. We use the Hi-net records surrounding the hypocenters and solve a linear system defined by the representation theorem for seismic sources using non-negative least squares method (Lawson and Hanson, 1974). Our result demonstrates that both ruptures initiate in a similar way until approximately 0.2 s after the nucleations. For the foreshock, the rapid growth completes at about 0.2 s which is consistent with T_{dp} and the duration of the “growth stage” (Uchide and Ide, 2010). On the other hand, for the mainshock, it continues to grow up rapidly even after 0.2 s. We consider that this variation in initiating process may have resulted in the difference of the final sizes.

Keywords: Initial rupture, Nucleation, The 2016 central Tottori earthquake, Slip inversion, Kinematic modeling, Deterministic property

Simultaneous estimation of the dip angles and slip distribution on the two active faults of the 2016 Kumamoto earthquak

*Yukitoshi Fukahata[1], Manabu Hashimoto[1]

1. Disaster Prevention Research Institute, Kyoto University

At the 2016 Kumamoto earthquake, surface ruptures were observed not only along the Futagawa fault, where main ruptures occurred, but also along the Hinagu fault. To estimate the slip distribution on these faults, we extend a method of non-linear inversion analysis (Fukahata and Wright 2008) to a two-faults system. With the method of Fukahata and Wright (2008) we can simultaneously determine the optimal dip angle of a fault and the slip distribution on it, based on Akaike's Bayesian Information Criterion (ABIC) by regarding the dip angle as an hyperparameter. By inverting the InSAR data with the developed method, we obtain the dip angles of the Futagawa and Hinagu faults as 61º ±6º and 74º ±12º, respectively. The slip on the Futagawa fault is mainly strike slip. The largest slip on it is over 5 m around the center of the model fault (130.9º in longitude) with a significant normal slip component. The slip on the Futagawa fault quickly decreases to zero beyond the intersection with the Hinagu fault. On the other hand, the slip has a local peak just inside Aso caldera, which would be a cause of severe damage in this area. A relatively larger reverse fault slip component on a deeper part around the intersection with Aso caldera suggests that something complicated happened there. The slip on the Hinagu fault is almost a pure strike slip with a peak of about 2.4 m. The developed method is useful in clarifying the slip distribution, when a complicated rupture like the Kumamoto earthquake happens in a remote area.

Keywords: The 2016 Kumamoto earthquake, weak nonlinear inversion analysis, ABIC

Rupture processes of the 2016 Kumamoto earthquake sequence: Causes for extreme ground motions

*Hiroaki Kobayashi[1], Kazuki Koketsu[1], Hiroe Miyake[2,1]

1. Earthquake Research Institute, The University of Tokyo, 2. Interfaculty Initiative in Information Studies, The University of Tokyo

The 2016 Kumamoto earthquake sequence including three large events (M6.5 on April 14, M6.4 on April 15, and M7.3 on April 16) caused severe damage to the Kumamoto prefecture and surrounding region. During the M7.3 event, extreme pulse-like velocity waveforms were observed in the town of Mashiki and the village of Nishihara. To investigate the rupture processes of the 2016 Kumamoto earthquake sequence and causes for these pulse-like waveforms, we performed the joint source inversions of the three notable events using strong motion, teleseismic, and geodetic data.
We constructed multi-segment faults models for the three events. We first relocated the hypocenters of the sequence by double difference method [Waldhauser and Ellsworth, 2000]. Considering the relocated hypocenters distributions, focal mechanisms, and active faults, we divided the source region into four regions. Four regions correspond to the Hinagu fault zone, the junction of the Futagawa and Hinagu fault zones, the Futagawa fault zone, and the inner Aso caldera. We also adjusted the one-dimensional velocity structure models for strong motion stations using five medium-sized earthquakes.
The obtained results are following: 1) The M6.5 event initiated on southeast dipping fault and then ruptured the Hinagu fault toward southwest; 2) The M6.4 event initiated on the Hinagu fault and ruptured the adjacent region to the M6.5 rupture area; 3) The M7.3 event initiated on the deep part of the Hinagu fault and propagate to northeast along the Futagawa fault; 4) Extreme ground motion observed in the town of Mashiki and the village of Nishihara can be attributed to the event's upward rupture directivity and fast slip rate.

Keywords: 2016 Kumamoto earthquake, rupture process, joint inversion

Dynamic rupture simulation of two cascading foreshocks of the 2016 Kumamoto earthquake

*Hiroki Arai[1], Ryosuke Ando[2], Yosuke Aoki[3]

1. Faculty of Science, University of Tokyo, 2. Graduate School of Science, University of Tokyo, 3. Earthquake Research Institute, University of Tokyo

The 2016 Kumamoto earthquake sequence, including two major foreshocks (Mw 6.2 and 6.0) and the main shock (Mw 7.0), hit the Kyushu island of southwest Japan. The foreshocks have a temporal separation of approximately 2.5 hours; the latter one has apparently been triggered by the former one by its change in static stress, dynamic stress, or both. We assumed that those foreshocks had ruptured subparallel but different faults on the Hinagu fault system, and constructed a dynamic model to gain insights into the mechanism of such consecutive events by computing the temporal evolution of stress and slip rate on both faults using Boundary Integral Equation Method. Our results show that, under circumstances satisfying local stress field constrained by an independent information of spatial variations of earthquake focal mechanisms, the rupture of former foreshock dynamically triggered the second foreshock. In addition, parameter studies gave us indication of the relationship between local frictional properties and stress filed. Our result is also consistent with observed ground deformation from the ALOS-2 Synthetic Aperture Radar satellite.

Keywords: Dynamic rupture simulation, Kumamoto Earthquake, Synthetic Aperture Radar

3-D Dynamic Rupture Simulations of the 2016 Kumamoto, Japan, Earthquake

*Yumi Urata[1], Keisuke Yoshida[2], Eiichi Fukuyama[1]

1. National Research Institute for Earth Science and Disaster Resilience, 2. Tohoku University

Using 3-D dynamic rupture simulations, we investigated the 2016 M7.3 Kumamoto, Japan, earthquake to illuminate why and how the rupture of the main shock propagated successfully, assuming a complicated fault geometry estimated on the basis of the distributions of the aftershocks. The M7.3 main shock occurred along the Futagawa and Hinagu faults. A few days before, three M6-class foreshocks occurred. Their hypocenters were located along the Hinagu and Futagawa faults, and their focal mechanisms were similar to those of the main shock; therefore, an extensive stress shadow may have been generated on the fault plane of the main shock. First, we estimated the geometry of the fault planes of the three foreshocks as well as that of the main shock based on the temporal evolution of the relocated aftershock hypocenters. We then evaluated the static stress changes on the main shock fault plane that were due to the occurrence of the three foreshocks, assuming elliptical cracks with constant stress drops on the estimated fault planes. The obtained static stress change distribution indicated that the hypocenter of the main shock was located in the region with a positive Coulomb failure stress change (ΔCFS), while the ΔCFS in the shallow region above the hypocenter was negative. Therefore, these foreshocks could encourage the initiation of the main shock rupture and could hinder the propagation of the rupture toward the shallow region. Finally, we conducted 3-D dynamic rupture simulations of the main shock using the initial stress distribution, which was the sum of the static stress changes caused by these foreshocks and the regional stress field. Assuming a slip-weakening law with uniform friction parameters, we conducted 3-D dynamic rupture simulations by varying the friction parameters and the values of the principal stresses. We obtained feasible parameter ranges that could reproduce the characteristic features of the main shock rupture revealed by seismic waveform analyses. We also demonstrated that the free surface encouraged the slip evolution of the main shock.

Dynamic rupture simulation with complex fault geometries for the 2016 Kaikoura, New Zealand, earthquake

*Ryosuke Ando[1], Yoshihiro Kaneko[2]

1. Graduate School of Science, University of Tokyo, 2. GNS Science

The 2016, Mw 7.8, Kaikoura earthquake is a unique event with its rupture process that propagated through the significantly complicated fault system, suggested according to field surveys and an Interferometric synthetic aperture radar InSAR observation (Hamling et al., 2017, submitted). The InSAR observation infers up to 19 fault segments, where some of them are newly identified. Since the fault geometry is considered as one of primary parameters controlling the initiation, propagation and termination of earthquake ruptures, it is important to understand which conditions allow the rupture to propagate through multiple fault segments having such complicated geometries. In this study, we apply the dynamic rupture simulation to reproduce the observed rupture processes and slip distributions. For the numerical analysis, we employ the spatio-temporal boundary integral equation method with the fast domain portioning method (FDPM), which enables us the accurate and efficient analyses of the nonplanar fault geometry. The fault model is developed by referring Hamiling et al. (2017). The regional stress field is determined based on the seismological stress tensor inversion done previously in this region (Balfour et al., 2005, GJI). The observationally constrained stress axes were consistent with the overall dextral faulting of the NE-SW trended fault systems but locally some fault segments appear to be obliquely oriented. The preliminary computation shows that the distribution of the tractions resolving the regional stress on each fault segment was largely varied over the fault system, suggesting to cause the complex rupture process.

Keywords: Dynamic rupture simulation, Boundary integral equation method, Complex fault geometry

Strain rate effect on rupture nucleation and mainshock propagation speed

*Shiqing Xu[1], Eiichi Fukuyama[1], Futoshi Yamashita[1], Kazuo Mizoguchi[2], Shigeru Takizawa[1], Hironori Kawakata[3]

1. NIED, Japan, 2. CRIEPI, Japan, 3. Ritsumeikan Univ.

Multiple lines of evidence have indicated that the same fault portion can host a diverse spectrum of deformation modes. They include the coexistence of pseudotachylite and mylonite near the base of the seismogenic zone, the coexistence of slow slip and unstable rupture in the Japan Trench as well as in the laboratory, and the transient deepening of seismicity below the normal brittle-to-ductile transition depth after a major earthquake. In addition to pressure-temperature condition and material composition, strain rate has been invoked to explain the diversity and switch of deformation modes of solids. In this work, we investigate how strain rate may affect the behavior of fault slip, based on direct shear experiments using meter-scale rock samples made of Indian metagabbro (nominal fault area is 1.5 m x 0.1 m). In addition to the macroscopic frictional behavior measured by load cells, we monitor the local fault behavior utilizing a high-density array of strain gauges mounted close to the synthetic fault (20-40 mm off the fault). We conduct experiments under a constant normal stress of 6.7 MPa, and a constant loading rate ranging from 0.01 mm/s to 1 mm/s. For the highest loading rate, we focus on the early part right after the initial running-in stage, during which fault surface condition has not been significantly altered. We approximately evaluate the strain rate by referring to the applied loading rate over a fixed sample size, while also point out that the actual local strain rate can greatly fluctuate depending on the ongoing deformation mode. Our macroscopic observation shows that for all the tested cases the fault motion is characterized by stick-slip, implying an overall brittle faulting regime. Detailed local observation reveals that quasi-stable slow slip phase preceding unstable mainshocks is a common feature for cases under a low loading rate (e.g. 0.01 mm/s), but can be skipped (below the 50-mm resolution of our strain gauge array) under a high loading rate (e.g. 1 mm/s). Another related local observation is that mainshock propagation speed is often faster under a higher loading rate, possibly exceeding the shear wave speed of metagabbro (i.e. supershear rupture). Based on the well-known theoretical result that the balance between elastic strain energy and fracture energy controls the critical transition length scales and rupture speed (Madariaga and Olsen, 2000), we suggest the following ideas for understanding our laboratory observations. (1) High-rate loading can more efficiently transfer energy to the rock bulk, and the average stress level operating over the entire fault can well exceed that set by the weakest fault patch. (2) High-rate loading can enhance the brittleness of fault rocks by reducing the apparent fracture energy (Freund, 1990): some inelastic process will not have enough time to dissipate energy before the failure criterion is reached near a rapidly stressed rupture front. It should be noted that the above point (2) is not always true, as in other circumstances high-rate loading can cause an increase in the apparent fracture energy through mechanisms such as rupture bifurcation, intense microcracking, and gouge generation. When these scenarios occur, rupture propagation may strongly fluctuate or even get arrested. Therefore, more investigations are needed to categorize strain rate effect during different stages of fault slip.

Keywords: Strain rate, Rupture nucleation, Mainshock propagation

Supershear rupture induced by step over geometry

*Feng Hu[1], Hengxin Ren[2], Xiaofei Chen[1,2]

1. Univ. of Sci. &Tech. of China, 2. Srn. Univ. of Sci. & Tech.

Based on dynamic rupture simulations on strike-slip step overs in a 3-D full space where the initial shear stresses preclude a supershear transition according to the Burridge-Andrews supershear transition mechanism, we show that rupture speeds can transit from subshear on the primary fault to supershear on the secondary fault for both compressional and extensional step overs. The low normal stress zone and the high shear stress zone, which radiate from the end of the primary fault if its rupture arrest is sudden, coincides beyond the fault step, and determine the supershear rupture occurrence on the secondary fault. However, a low shear stress zone traveling at the shear wave speed is also radiated, making the rupture speed return to subshear in most cases. Sustained supershear rupture are also possible on compressional step overs under certain conditions. Self-arresting ruptures are observed in the overlap area on the secondary fault. In the homogeneous half-space model where supershear rupture exists on the primary fault, because of the free-surface, the rupture speed on the secondary fault rapidly transits to subshear near the fault step if its width exceeds a critical value. The distribution of peak ground velocities are also investigated.

Keywords: supershear ruptures can be induced by a fault step over, stress waves radiated from the end of the primary fault control supershear transition on secondary fault segments, rapid rupture speed transitions at step overs in a half-sapce

Synchronization of Stick-Slip Oscillator by Periodic External Forces -Elastic and Viscoelastic Cases-

*Kazuro Hirahara[1]

1. Department of Geophysics, Earth and Planetary Sciences, Graduate School of Sciences, Kyoto University

In the last JpGu meeting, I reported the responses of stick-slip oscillator to periodic external forces. There, I examined the quasi-dynamic motion of a block connected with a spring pulling with a constant loading rate vpl, where the laboratory-derived rate- and state-friction law is working on the contact surface between the block and the underlying floor. I used frictional parameters a, b, L appropriate for velocity weakening and the spring constant k less than a critical stiffness kc to produce a repeating stick-slip motion of the block, which is a simple earthquake cycle model with a recurrences time. Then, I applied periodic external forces with several periods and observed clear m:n synchronization phenomena with synchronization frequency (period) widths, which is so called ‘Devil’s Staircase’. Here, fe:fc (Tc:Te)=m:n (m and n are coprime integers) where fe and fc (Tc and Te) are frequencies (periods) of the external force and the simulated system, respectively.

This paper is a continuation of the previous one. The m:n synchronization is clear for the external force with the amplitude larger than 10 or 1 percent of stress drop during an earthquake cycle. At first, I supposed to use this synchronization for explaining the observed statistical significance of periodicity and seasonality of seismic activities. The stress changes of periodic daily and long-term tidal forces is an order of kPa. The amplitude of stress drop for usual earthquakes and slow slip events (SSEs) is an order of MPa and kPa. Then tidal forces can contribute to synchronization of SSEs, but not of usual earthquakes. But a simulation study shows a possible existence of long-term SSE with a larger stress drop of 0.1 MPa, which causes synchronization of large earthquakes such as those along the Nankai trough. The other extension is to investigate viscoelastic cases. The elastic spring is replaced by the standard linear solid, where the elastic spring with k1 and the Maxwell viscoelastic element (a spring with k2 is serially connected with a dash-pot of viscosity eta) are connected in parallel, and the relaxation time is tr=k2/eta. The change of relaxation time tr causes the recurrence times. And I discuss the synchronization in these viscoelastic cases, comparing with the elastic cases.

Keywords: Stick-Slip Oscillator, Synchronization, Rhythm, Earthquake Cycle Simulation , Periodic External Force, Elastic and Viscoelastic

Physics-based simulation for possible interplate earthquakes along the Nankai trough

*Chihiro Hashimoto[1], Yumi Urata[2], Eiichi Fukuyama[2]

1. Graduate School of Environmental Studies, Nagoya University, 2. National Research Institute for Earth Science and Disaster Resilience

In order to numerically generate possible earthquake scenarios for the Eurasian-Philippine Sea plate interface along the Nankai trough in southwest Japan, we need to assimilate diverse observation data into a physics-based 3-D model of earthquake generation cycles. Hashimoto *et al.* (2014) developed a numerical simulation system which consists of the quasi-static tectonic loading model and the dynamic rupture propagation model, based on the common 3-D model of plate interface geometry. In the theoretical framework of this system, our problem is to simulate time evolution of stress states so that the past slip history at plate interfaces estimated from observation data is adequately reproduced. Given the stress state and fault constitutive relation just before the earthquake occurrence, we can compute the subsequent rupture propagation process. In the numerical methods to reproduce realistic stress states and to generate possible earthquake scenarios, it is essential to assign a proper fault constitutive relation to control both the processes of quasi-static tectonic loading and dynamic rupture propagation. In the present study, we use the slip- and time-dependent fault constitutive law proposed by Aochi and Matsu'ura (2002), where time evolution of macroscopic relation between fault slip and shear strength is prescribed by the abrasion rate and the adhesion rate of microscopic fault surface topography and a constant representing mechanical properties of the contact zone, and therefore we need to examine distribution of these parameters. Interseismic increase rates of slip deficit along the Nankai trough inferred from GPS data inversion are used to constrain the constitutive parameters and to verify the numerical results. The sequence of the past large interplate earthquakes and their rupture initiation points and coseismic slip distributions are also used. Setting proper distribution of the constitutive parameters, we can generate possible earthquake scenarios with the method developed by Hok *et al.* (2011), which enables us to discuss potential earthquakes along the Nankai trough in terms of stress states at the moment and the relevant possible dynamic ruptures under inherent stress disturbances.

Sea-surface Displacement and Tsunami Inundation Including Seismic Waves and Tsunami for Anticipated Nankai Trough Earthquakes, Southwest, Japan

*Tatsuhiko Saito[1], Toshitaka Baba[2], Shunsuke Takemura[1], Eiichi Fukuyama[1]

1. National Research Institute for Earth Science and Disaster Resilience, 2. Graduate School of Science and Technology, Tokushima University

When observation stations are located apart from an earthquake hypocenter, tsunami arrives much later than seismic waves because tsunami propagates considerably slower than seismic waves. Hence, we effortlessly exclude seismic waves by just setting an appropriate time window when we analyze tsunami signals. However, when analyzing the waveforms recorded inside the focal area, it is difficult to decompose the wavefield into seismic waves and tsunami. We need to employ a theory that describes seismic waves and tsunami simultaneously. For example, Saito and Tsushima (2016) proposed a method for synthesizing ocean-bottom pressure records considering both seismic waves and tsunami. They evaluated the performance of a real-time tsunami forecasting algorithm called tFISH (e.g., Tsushima et al. 2012) by using the synthesized records.
New observation networks such as DONET and S-net are designed for the observation inside the focal area. Therefore, it is fundamentally important to investigate the contributions of seismic waves in tsunami waveforms. Recent development of tsunami observation technology enables us to observe tsunami not only by sea-bottom pressure change but also by sea-surface displacement by using GPS buoys. Inazu et al. (2016) showed that real-time tsunami source estimation is possible if we utilize high-precision, real-time GPS height observations equipped with cargo ships and tankers. At present, a method for synthesizing ocean-surface displacement including both seismic waves and tsunami is urgently required. The present study proposes a method that calculates both the sea surface displacement including seismic waves and tsunami in addition tsunami inundation along coasts. Taking the anticipated Nankai-Trough huge earthquakes as example, we theoretically created the sea-surface displacement waveforms and the inundation. We used the scenarios proposed by Hok et al. (2011) where the earthquake ruptures were simulated based on the friction law established in laboratory experiments and the slip deficit distribution estimated by geodetic-data analysis. By using their rupture scenarios as seismic sources in 3-D seismic-wave propagation simulations, we calculated spatial and temporal variation of the sea-surface displacement field without considering gravity (e.g., Takemura et al. 2016). Then, we included the contribution of gravity to the displacement field (in other words, simulated surface-height propagation as tsunami) by numerically solving nonlinear long-wave tsunami equations. We successfully simulated the inundation process with high-resolution topography data (minimum grid-spacing is ~6 m) by integrating a code referred to as JAGRUS (Baba et al. 2015) to the scheme proposed in this study.
Seismic waves and tsunami simultaneously appeared in the sea-surface displacement during the earthquake rupture, which can be noise for tsunami analyses. The seismic wave contribution to sea-surface displacement was smaller than to the sea-bottom pressure change. Since the moment rate becomes larger when the rupture duration gets shorter, seismic wave contributes more due to shorter rupture duration. On the other hand, tsunami inundation is mainly controlled by the moment but not the moment rate. The data sets created in this study would be useful for practical tests of tsunami-prediction algorithms using sea-surface displacement waveforms.

Keywords: Seismic Wave, Tsunami, Simulation

Observation and simulation of the regional-distance S-PL wave from the very deep (h=680 km) Mw 7.9 Ogasawara Islands earthquake of 2015 May 30

*Takashi Furumura[1], Brian L N Kennett[2]

1. Earthquake Research Institute The University of Tokyo, 2. Research School of Earth Sciences The Australian National University

Deep earthquakes in the subducting Pacific slab frequently produce anomalously large ground motions over Japan along the east coast of Honshu due to an efficient slab waveguide effect for high-frequency (f >1 Hz) signals caused by multiple forward scattering in heterogeneous and high-Q slab.

A recent observation of the Mw 7.9 earthquake beneath the Ogasawara Islands on 2015 May 30 at 680 km depth, produced an anomalously large shock over Japan with a distinctive pattern of ground motion with significantly stretched shaking intensity contours from the hypocenter to northern Honshu along the Pacific seaboard, demonstrated a typical pattern of the deep Pacific slab events.

However, the observed waveforms of regional distances (D=1000-2000 km) recoded by the F-net broadband, strong motion instruments indicate that the large ground acceleration arises from relatively low-frequency (f < 1 Hz) S-wave pulses and following low-frequency (f < 0.1 Hz) signals with long tails. The arrival of the slab-guided high-frequency signal was very late and weak compared with ordinary slab events. Such an anomalous wavefield may arise due to the very great depth of this event, about 100 km deeper than other seismicity in the vicinity.

Numerical simulation of seismic wave propagation employing the 3-D finite-difference method with a detailed structural model of the Pacific slab subduction zone shows how the deep source affects the regional wavefield. The results of the simulation demonstrate that the S waves radiating from the very deep (h=678 km) source out of the slab travel upwards and impinge on the crust at around 1000 km epicentral distance with similar slowness to P in the crust to produce strong S-to-P conversions at the free surface. The converted P waves are trapped in the crust with multiple Moho and surface reflections interfering to produced a long-period PL wave. Such a PL wave developed from a very deep source can travel substantial distances with successively supply of S wave from depth to the crustal waveguide for distances to 2000 km. Also the incidence of the S waves with the same slowness as the PL wave traveling in the crust makes a shear-coupled PL (S-PL) wavetrain with long-period (T=5-10 s). Later, weak slab-guided S waves from the very deep event are also transferred injected into the crust and continue as an Lg wave traveling in the crustal waveguide.

Though the S-PL wave is often noticed in the teleseismic (D=50-60 deg.) records as a dispersed long-period (T=20-30 s) wavetrains following the S and SS waves, this study demonstrates that the S-PL wave can be also developed in the regional distances (D=10-20 deg.) from very deep sources. However, the visibility of the regional S-PL phases depends strongly on the development of the high-frequency slab-guided waves, which can entirely override the regional seismic wavefield along the slab. The clear observation of the regional S-PL wave from the very deep earthquake beneath Ogasawara Island is because this event occurred out of the main slab.

Keywords: Simulation, 2015 Ogasawara earthquake, SPL wave , Deep-focus earthquake

